Journal of Sound and Vibration (2000) **236**(5), 761–779
doi:10.1006/jsvi.1999.2993, available online at http://www.idealibrary.com on IDEAL®

CANCELLATION OF MASS-LOADING EFFECTS OF TRANSDUCERS AND EVALUATION OF UNMEASURED FREQUENCY RESPONSE FUNCTIONS

J. M. M. Silva, N. M. M. Maia and A. M. R. Ribeiro

Department of Mechanical Engineering, Instituto Superior Técnico, Av. Rovisco Pais, 1049-001 *Lisboa, Portugal. E-mail: d569@beta.ist.utl.pt*

(*Received* 9 *June* 1999, *and in final form* 20 *October* 1999)

The problem of the cancellation of mass-loading effects of transducers in experimental structural dynamic analysis is addressed. A generalized solution based upon dynamic coupling and uncoupling of substructures is presented. It is shown that it is possible to solve the problem, no matter where the extra loading masses are located, by means of a series of relatively straightforward calculations. It is also shown that one can obtain frequency response functions (FRFs) without having to undertake the corresponding measurements. Up to now, the problem of obtaining the dynamic properties of all the structure FRF curves has only been considered possible provided the complete FRF matrix has been measured. The purpose of this paper is to contribute to solving this problem. In fact, the technique developed for cancellation of mass-loading effects is shown to also allow for the evaluation of the complete FRF matrix. A simple numerical example is presented to illustrate the good theoretical performance of the method. The same example is extended to incorporate noise, simulating an experimental situation, and it is shown that the technique is highly sensitive to measurement inaccuracies and that further work is necessary in order to solve this difficulty. A possible solution to improve the results is presented and discussed.

1. INTRODUCTION

Assuming a system with N degrees of freedom, hysteretically damped, it is easy to show [1, 2] that is dynamic characteristics may be described by an $N \times N$ receptance matrix of frequency response functions $\alpha_{jk}(\omega)$ relating the response at a given co-ordinate j to an excitation force applied at a given co-ordinate k. Each element $\alpha_{jk}(\omega)$ of the receptance matrix can be expressed by

$$\alpha_{jk}(\omega) = \sum_{r=1}^{N} \frac{\phi_{jr}\phi_{kr}}{(\omega_r^2 - \omega^2 + \mathrm{i}\eta_r\omega_r^2)}, \tag{1}$$

where $\mathrm{i} = \sqrt{-1}$, ϕ_{jr} and ϕ_{kr} are elements j and k of the mass-normalized mode shape vector of mode r, ω is the current excitation frequency and ω_r and η_r are the rth mode natural frequency and hysteretic damping factor respectively. Equation (1) is frequently written in the form

$$\alpha_{jk}(\omega) = \sum_{r=1}^{N} \frac{{}_r\bar{A}_{jk}}{(\omega_r^2 - \omega^2 + \mathrm{i}\eta_r\omega_r^2)}, \tag{2}$$

0022-460X/00/400761 + 19 $35.00/0

where

$$ {}_r\bar{A}_{jk} = \phi_{jr}\phi_{kr} = {}_rA_{jk}\mathrm{e}^{\mathrm{i}\,{}_r\varphi_{jk}} \tag{3} $$

is a complex quantity known as the modal constant, for which

$$ {}_rA_{jk} = |\phi_{jr}\phi_{kr}|, \qquad {}_r\varphi_{jk} = \arg(\phi_{jr}\phi_{kr}) \tag{4} $$

are constants for a given r, j and k. Two important conclusions can be extracted from the above equations. First, it is clear that the receptance matrix is symmetric and therefore

$$ \alpha_{jk}(\omega) = \alpha_{kj}(\omega), \tag{5} $$

this property being known as the principle of reciprocity and second, the modal constants are interrelated, obeying a relationship that is described by the pair of equations

$$ {}_r\bar{A}_{jk} = \phi_{jr}\phi_{kr}, \qquad {}_r\bar{A}_{jj} = \phi_{jr}^2 \quad \text{or} \quad {}_r\bar{A}_{kk} = \phi_{kr}^2, \tag{6} $$

known as the modal constants consistency equations. What equations (5) and (6) mean is that if a full row (or column) of the receptance matrix $[\alpha(\omega)]$, is known, then the whole matrix can be evaluated. Unfortunately, in practical situations, only an incomplete number of modes can be included in the analysis, the frequency range of the experimental analysis being limited. The response model will therefore be truncated and contain errors due to omission of all the out-of-range modes. One way of minimizing the consequences of using such a model is to introduce corrections on the FRFs so that they approximate the measured data in the frequency range of interest, by including an extra term in the response equation, i.e.,

$$ \alpha_{jk}(\omega) = \sum_{r=1}^{N_{inc}} \frac{{}_r\bar{A}_{jk}}{(\omega_r^2 - \omega^2 + \mathrm{i}\eta_r\omega_r^2)} + \bar{R}_{jk}(\omega), \tag{7} $$

where $\bar{R}_{jk}(\omega)$ is a complex residual term accounting for the contribution of the out-of-range modes and $N_{inc} < N$ is the incomplete number of modes included in the analysis. This residual term does not obey any consistency relationships such as the ones described by equations (6) and therefore, estimating unmeasured FRFs from the measured ones (one row or one column of the FRF matrix) is not accurate unless values for the relevant residual terms can be estimated. In the past, some effort has been made [3] to relate the residual effects of out-of-range modes between measured and unmeasured FRFs, but without much success in the sense of drawing general conclusions.

Moreover, measurement of the dynamic response of a structure, in terms of frequency response functions (FRFs), often involves the use of accelerometers and force transducers and therefore one measures directly the accelerance $H(\omega)$ instead of the receptance $\alpha(\omega)$. This poses no problem as accelerance and receptance are just two different forms of presenting the same FRF, and can be simply related by

$$ H(\omega) = -\omega^2\alpha(\omega). \tag{8} $$

However, the use of transducers such as the accelerometers and force gauges, imply changes in the measured FRFs due to the loading of the structure with extraneous (though sometimes negligible) masses. Figure 1(a) illustrates a typical FRF measurement set-up where the measurement of a direct FRF on a free–free beam is to be performed. One can

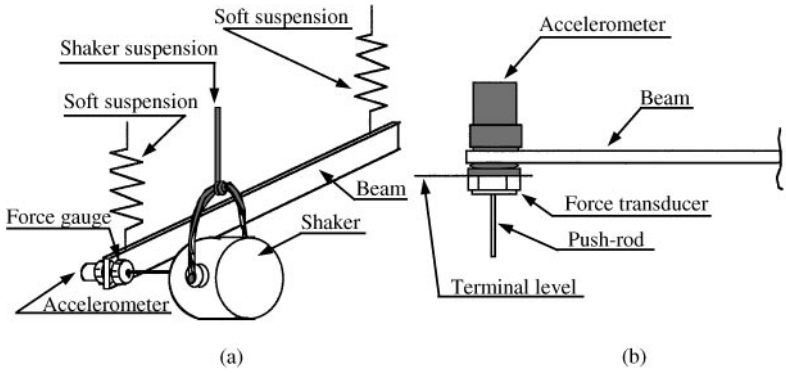

Figure 1. (a) Schematic representation of the test set-up for measuring a direct FRF on a free–free beam; (b) beam and transducers, the shadowed zone representing the total extra mass m, contributing to the measured force signal.

observe the shaker and the transducers (force gauge and accelerometer) capturing the force excitation and the acceleration response signals. The effective accelerance FRF of the beam at that point is to be determined; i.e., the relation

$$H = \frac{\ddot{x}}{f} \tag{9}$$

for the entire experimental frequency range, where $\ddot{x}$ is the beam acceleration response and f is the force effectively applied to the beam at that point, as if there were no interference caused by the addition of transducers to the system under consideration. However, the use of an experimental set-up such as the one shown in Figure 1(a) allows only for the measurement of an accelerance FRF (H_{meas}) of the system which includes both the beam and the additional mass of the transducers (obviously, it is assumed that the transducers behave as rigid bodies within the frequency range of interest). It is easy to see that, in this case, to obtain an acceleration response signal $\ddot{x}$, which is the actual acceleration of the beam, the input force excitation is not the true force one requires for the calculation of H, as in equation (9). This is due to the fact that part of the force supplied by the shaker is spent on accelerating part of the force transducer mass and also the accelerometer mass, as shown in Figure 1(b). Only about half of the force transducer mass contributes to the force signal, because the terminal is nearly at half the thickness of the transducer (note that this is only true for the direction that is considered. For directions perpendicular to the one under consideration all the force transducer mass has to be taken into account). The shadowed zone in Figure 1(b) represents the total extra driven mass, m.

As the objective is to obtain the effective force f applied to the beam, one must subtract from the measured force f_{meas} the inertia force corresponding to the total extra mass m, i.e.,

$$f = f_{meas} - m\ddot{x}. \tag{10}$$

Dividing equation (10) by $\ddot{x}$, it follows that

$$\frac{f}{\ddot{x}} = \frac{f_{meas}}{\ddot{x}} - m \qquad \text{or} \quad \frac{1}{H} = \frac{1}{H_{meas}} - m, \tag{11, 12}$$

where H_{meas} is the measured accelerance FRF. From equation (12), one obtains the desired accelerance FRF:

$$H = \frac{H_{meas}}{(1 - mH_{meas})}. \tag{13}$$

This process is known as mass cancellation [1, 2]. In general terms, it is important to proceed in this way whenever the extra masses are significant with respect to the structure mass itself, although this should be preferably regarded from the point of view of the modal masses associated with the structure. In fact, in a given frequency range, the structure exhibits a number of resonances for each of which there is an associated modal mass. If the mass of the transducers is significant by comparison with a particular modal mass, then the measured resonant frequency will be lower than its true value. On the other hand, if the extra mass is close to a node, no important effect is expected (provided no rotational inertia is being accounted for).

In general, some of the resonances will always be affected somewhat by the masses of the transducers, so a mass cancellation procedure is usually desirable, especially if the accelerometer position is to be moved around the structure, which is often the case. As shown above, the mass cancellation procedure is quite straightforward when one is dealing with direct point FRFs; one must simply apply expression (13). However, if one wishes to undertake mass cancellation in transfer FRFs, there was not, until very recently, any specific technique available. In fact, McConnell [4] presented a partial solution, where the mass added at the excitation point could be cancelled, but not the mass added at the response location. The authors addressed this problem a few years ago [5, 6] and proposed a possible solution that was further developed and discussed 1 year later by Ashory [7]. The initial purpose of this paper is to show that the generalization of the mass cancellation principle to any transfer FRF is indeed (at least, theoretically) possible. On the other hand, as will be shown, the process of evaluating the whole FRF matrix from measurements taken on a single column (or row) is shown to be a consequence of the solution of the mass cancellation problem.

It is worth mentioning now that, in any real case (which is a 3-D problem), an added mass at a given point of the structure will obviously introduce changes due to translational and rotational inertias in all six possible directions of motion of its centre of gravity. A point mass modification that is effective in a single degree of freedom is only achieved by use of very special attachment methods that are not normally employed for fixing response transducers. The complete problem is therefore much more difficult to solve. In this paper, it is assumed that the added mass effect considered to be important is only related to the translation response in the direction of the transducer sensitivity axis, all the other being assumed negligible.

A similar reasoning may be applied to the force transducer as, in fact, it will also add mass (and rotational inertia) to the structure in more than a single degree of freedom. In this case, however, there is a subtle difference in the effective point masses added for a force transducer that does not occur with an accelerometer. It is true that the effective mass of a force transducer that is added to a structure in the direction of the excitation force is given by the base-side mass that is usually between one-third and one-half of the mass of the transducer. However, in directions perpendicular to the excitation direction, the full mass of the force transducer is added to the structure. Again, for the purpose of this paper, it is assumed that the added mass effect considered to be important is only related to the excitation direction of the transducer, all the others being assumed to be negligible.

The procedure is summarized in this paper, recalling the various necessary steps already presented in previous work [5, 6]. It is shown, using a very simple system, that the method works perfectly well when an exact numerical example is used. However, it is also shown that the method is highly vulnerable to inaccuracies in the FRF data, using the same numerical example polluted by random noise (to simulate an experimental situation). The reasons for this error sensitivity are addressed and discussed. It is shown that results can be dramatically improved if an auxiliary stiff spring (or large mass) is used during the experimental procedure and cancelled out by post-processing the data. Though the proposed solution may not be easy to implement in some situations, it performs well and opens a way for further studies that may lead to better solutions.

2. THEORETICAL DEVELOPMENT OF THE MASS UNCOUPLING METHOD (MUM)

2.1. BASIC EQUATIONS

Consider two substructures, A and B, that are rigidly connected through some co-ordinates at known common points, as shown schematically in Figure 2, together constituting structure C.

Continuing, let i represent the co-ordinates of interest for the analysis at points exclusively belonging to substructure A, k those exclusively belonging to substructure B and j the connection ones, i.e., those that are common to A and B, as schematically shown in Figure 2(b). Let also: $[\mathbf{H}_{ii}^{(A)}]$ represent the matrix of accelerance FRFs amongst co-ordinates i; $[\mathbf{H}_{ij}^{(A)}]$ represent the matrix of accelerance FRFs between co-ordinates i and j; $[\mathbf{H}_{jj}^{(A)}]$ represent the matrix of accelerance FRFs amongst co-ordinates j belonging to substructure A; $[\mathbf{H}_{kk}^{(B)}]$ represent the matrix of accelerance FRFs amongst co-ordinates k; and $[\mathbf{H}_{kj}^{(B)}]$ represent the matrix of accelerance FRFs between co-ordinates k and j.

Therefore, matrices $[\mathbf{H}^{(A)}]$ and $[\mathbf{H}^{(B)}]$ of the accelerance FRFs for each of the substructures A and B, will be given by the following expressions:

$$[\mathbf{H}^{(A)}] = \begin{bmatrix} [\mathbf{H}_{ii}^{(A)}] & [\mathbf{H}_{ij}^{(A)}] \\ [\mathbf{H}_{ji}^{(A)}] & [\mathbf{H}_{jj}^{(A)}] \end{bmatrix},$$
$$[\mathbf{H}^{(B)}] = \begin{bmatrix} [\mathbf{H}_{jj}^{(B)}] & [\mathbf{H}_{jk}^{(B)}] \\ [\mathbf{H}_{kj}^{(B)}] & [\mathbf{H}_{kk}^{(B)}] \end{bmatrix}. \tag{14}$$

The FRF matrix for the whole structure, $[\mathbf{H}^{(C)}]$, will be

$$[\mathbf{H}^{(C)}] = \begin{bmatrix} [\mathbf{H}_{ii}^{(C)}] & [\mathbf{H}_{ij}^{(C)}] & [\mathbf{H}_{ik}^{(C)}] \\ [\mathbf{H}_{ji}^{(C)}] & [\mathbf{H}_{jj}^{(C)}] & [\mathbf{H}_{jk}^{(C)}] \\ [\mathbf{H}_{ki}^{(C)}] & [\mathbf{H}_{kj}^{(C)}] & [\mathbf{H}_{kk}^{(C)}] \end{bmatrix}. \tag{15}$$

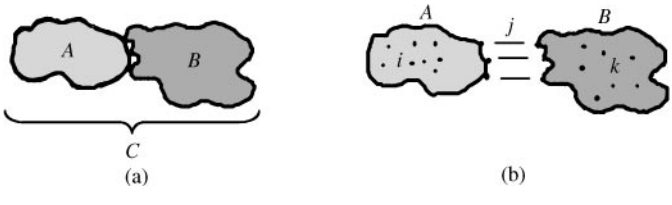

Figure 2. (a) Structure C, composed by two substructures A and B, connected together; (b) Notation for the sets of co-ordinates used.

Applying the appropriate equations of equilibrium and compatibility at the common points (and therefore at the common co-ordinates) that constitute the joining locations, the coupling of both substructures will result in a complete system C with an accelerance matrix given by the following equation [1, 2]:

$$[\mathbf{H}^{(C)}] = \left[\begin{bmatrix} \begin{bmatrix} [\mathbf{H}_{ii}^{(A)}] & [\mathbf{H}_{ij}^{(A)}] \\ [\mathbf{H}_{ji}^{(A)}] & [\mathbf{H}_{jj}^{(A)}] \end{bmatrix}^{-1} & \begin{bmatrix} \mathbf{0} \\ \mathbf{0} \end{bmatrix} \\ [\mathbf{0}] \quad [\mathbf{0}] & [\mathbf{0}] \end{bmatrix} + \begin{bmatrix} [\mathbf{0}] & [\mathbf{0}] & [\mathbf{0}] \\ [\mathbf{0}] & \begin{bmatrix} [\mathbf{H}_{jj}^{(B)}] & [\mathbf{H}_{jk}^{(B)}] \\ [\mathbf{H}_{kj}^{(B)}] & [\mathbf{H}_{kk}^{(B)}] \end{bmatrix}^{-1} \end{bmatrix} \right]^{-1}. \quad (16)$$

However, this formulation requires three matrix inversions, thus becoming computationally 'heavy" and often leading to poor conditioning problems. A simple way to improve the performance of the previous calculations is to perform some mathematical manipulations in equation (16), as shown by Skingle [8], and arrive at

$$[\mathbf{H}^{(C)}] = \begin{bmatrix} [\mathbf{H}_{ii}^{(A)}] & [\mathbf{H}_{ij}^{(A)}] & [\mathbf{0}] \\ [\mathbf{H}_{ji}^{(A)}] & [\mathbf{H}_{jj}^{(A)}] & [\mathbf{0}] \\ [\mathbf{0}] & [\mathbf{0}] & [\mathbf{H}_{kk}^{(B)}] \end{bmatrix} - \begin{bmatrix} [\mathbf{H}_{ij}^{(A)}] \\ [\mathbf{H}_{jj}^{(A)}] \\ -[\mathbf{H}_{kj}^{(B)}] \end{bmatrix}$$

$$([\mathbf{H}_{jj}^{(A)}] + [\mathbf{H}_{jj}^{(B)}])^{-1} ([\mathbf{H}_{ji}^{(A)}] \; [\mathbf{H}_{jj}^{(A)}] - [\mathbf{H}_{jk}^{(B)}]. \quad (17)$$

It is clear that this procedure not only involves a single matrix inversion (avoiding most of the usual numerical problems) but also the only inversion that is needed is of the order of the number of connecting co-ordinates j. For the purposes of this paper, an alternative form for equation (17) is proposed [5] and shall be used. Explicitly writing $[\mathbf{H}^{(C)}]$, it follows that

$$\begin{bmatrix} [\mathbf{H}_{ii}^{(C)}] & [\mathbf{H}_{ij}^{(C)}] & [\mathbf{H}_{ik}^{(C)}] \\ [\mathbf{H}_{ji}^{(C)}] & [\mathbf{H}_{jj}^{(C)}] & [\mathbf{H}_{jk}^{(C)}] \\ [\mathbf{H}_{ki}^{(C)}] & [\mathbf{H}_{kj}^{(C)}] & [\mathbf{H}_{kk}^{(C)}] \end{bmatrix} = \begin{bmatrix} [\mathbf{H}_{ii}^{(A)}] & [\mathbf{H}_{ij}^{(A)}] & [\mathbf{0}] \\ [\mathbf{0}] & [\mathbf{0}] & [\mathbf{H}_{jk}^{(B)}] \\ [\mathbf{0}] & [\mathbf{0}] & [\mathbf{H}_{kk}^{(B)}] \end{bmatrix} + \begin{bmatrix} -[\mathbf{H}_{ij}^{(A)}] \\ [\mathbf{H}_{jj}^{(B)}] \\ [\mathbf{H}_{kj}^{(B)}] \end{bmatrix}$$

$$([\mathbf{H}_{jj}^{(A)}] + [\mathbf{H}_{jj}^{(B)}])^{-1} ([\mathbf{H}_{ji}^{(A)}] \; [\mathbf{H}_{jj}^{(A)}] - [\mathbf{H}_{jk}^{(B)}]. \quad (18)$$

As it will be seen later, the latter formulation allows for a clearer visualization of the coupling and uncoupling procedure and of the interrelationship between the substructures FRFs. Either of expressions (17) and (18) allows for the calculation of the FRF system matrix of structure C, demanding a single inversion where the matrix to invert is of the order of the number of co-ordinates common to A and B. Therefore, one should expect that numerical problems and computational effort will have a far smaller significance than in the traditional way.

2.2. MEASUREMENT TECHNIQUE

The best way to explain how the proposed technique works is to use an example where a sequential procedure is applied. Hence, consider a structure X (Figure 3) with N co-ordinates of interest (hence, with N d.o.f.s for the purpose of the analysis). Suppose the intention is to characterize its dynamic behaviour, relating the N co-ordinates of interest

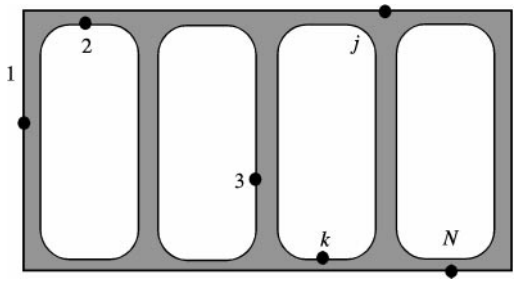

Figure 3. Schematic representation of the structure X to be studied, with N d.o.f.s.

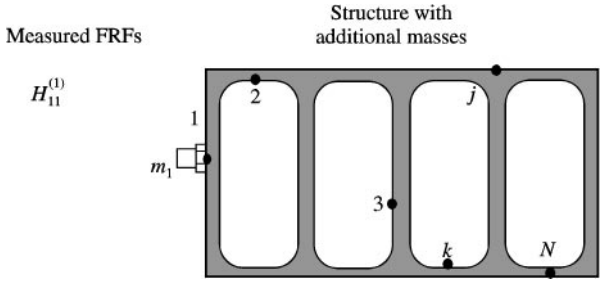

Figure 4. First measurement.

located, respectively, at points 1, 2, …, N, by measuring the corresponding FRFs. The structure will be excited with a shaker at a single co-ordinate, say no. 1, and the force and acceleration signals will be measured through a conventional force transducer and accelerometers. The measurements to be taken in order to cancel all the transducers added masses and obtain, at a later stage, the whole FRF matrix ($N \times N$) are the following (note that this sequential procedure is not mandatory; any alternative sequence can be used although the one presented allows for the implementation of a simple recursive algorithm):

1. Measure the direct FRF at co-ordinate 1 (Figure 4), where m_1 represent the added masses of the force transducer and of the accelerometer.
2. Add an accelerometer at co-ordinate 2 (mass m_2) and again measure the direct FRF at 1 and the transfer FRF relating 1 and 2 (Figure 5).
3. Add another accelerometer at co-ordinate 3 (mass m_3) and again measure the direct FRF at 1 and the transfer FRFs relating 1–3 (Figure 6).
4. Proceed as previously, adding an accelerometer at each new co-ordinate and performing the corresponding sets of measurements, ending with the last one (m_N) which is exemplified in Figure 7.

These are the complete sets of necessary measurements. It should be stressed that the shaker is always at co-ordinate 1 and that $(N^2 + N)/2$ measurements have been taken altogether. In fact, this number makes sense, as $(N^2 + N)/2$ unknown FRFs (the FRF matrix is $N \times N$ and symmetric) are being sought. If the number of d.o.f.s is too large and there are insufficient accelerometers, dummy masses may be used to replace them at positions tested already. In fact, dummy masses may always be used if there is a need to increase the

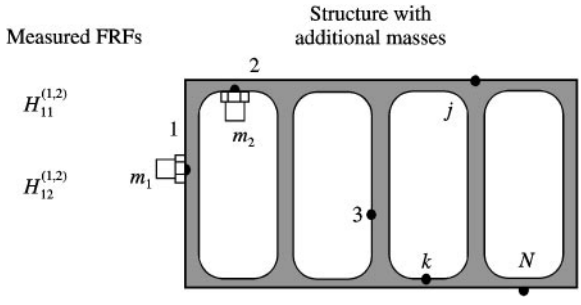

Figure 5. Second set of measurements.

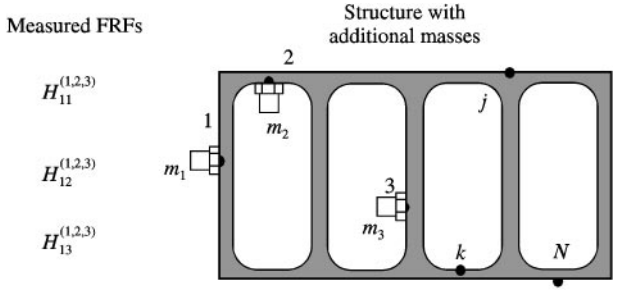

Figure 6. Third set of measurements.

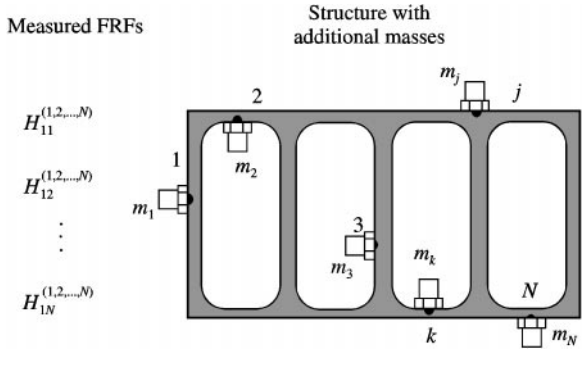

Figure 7. *N*th set of measurements.

perturbation effect of the extra masses (which might be advantageous for the particular case of this technique).

The following procedure is proposed, which is, in fact, very simple; for each situation corresponding to a set of measurements, the respective added masses will be uncoupled, in decreasing order. Starting with the first set of measurements, first uncouple mass 1, then for the second set uncouple mass 2 first and then mass 1, for the third set uncouple mass 3, then mass 2 and them mass 1, and so on. Note again that this sequential procedure is presented for the sake of clarity. It is always possible to use other sequences provided all extra masses are taken into account and all the needed FRFs are measured.

2.2.1. *First situation—uncoupling of* m_1

The structure represented in Figure 4 can be seen as the result of coupling X to m_1 and therefore, according to the substructure notation used in section 2.1 previously, it may be stated that

$$A \equiv X, \qquad B \equiv m_1, \qquad C \equiv X \oplus m_1,$$

where $\oplus$ means "coupled to". As N co-ordinates are being considered, the FRF matrix $[\mathbf{H}^{(A)}]$ will be of order N and $[\mathbf{H}^{(B)}]$ of order 1, as it represents a simple mass modification. The co-ordinates at points 2, 3, …, N correspond now to co-ordinates i, the co-ordinate at point 1 corresponds to co-ordinate j and, in this case, there is no co-ordinate k. The notation can be simplified further, replacing $\lfloor \mathbf{H}^{(A)} \rfloor$ by $[\mathbf{H}]$ (which is what is required) and $\lfloor \mathbf{H}^{(C)} \rfloor$ by $[\mathbf{H}^{(1)}]$, where the superscript (1) denotes the fact that there is now an additional mass (m_1) at co-ordinate 1. Noting that $H_{11}^{(B)} = 1/m_1$ is the only element in the FRF matrix $\lfloor \mathbf{H}^{(B)} \rfloor$ which is of order 1, equation (18) is then reduced to

$$\begin{bmatrix} \begin{bmatrix} H_{22}^{(1)} & H_{23}^{(1)} & \cdots & H_{2N}^{(1)} \\ H_{32}^{(1)} & H_{33}^{(1)} & \cdots & H_{3N}^{(1)} \\ \vdots & \vdots & & \vdots \\ H_{N2}^{(1)} & H_{N3}^{(1)} & \cdots & H_{NN}^{(1)} \end{bmatrix} \begin{Bmatrix} H_{21}^{(1)} \\ H_{31}^{(1)} \\ \vdots \\ H_{N1}^{(1)} \end{Bmatrix} \\ \{H_{12}^{(1)} \quad H_{13}^{(1)} \quad \cdots \quad H_{1N}^{(1)}\} \qquad \mathrm{H}_{11}^{(1)} \end{bmatrix} = \begin{bmatrix} \begin{bmatrix} H_{22} & H_{23} & \cdots & H_{2N} \\ H_{31} & H_{33} & \cdots & H_{3N} \\ \vdots & \vdots & & \vdots \\ H_{N2} & H_{N3} & \cdots & H_{NN} \end{bmatrix} \begin{Bmatrix} H_{21} \\ H_{31} \\ \vdots \\ H_{N1} \end{Bmatrix} \\ \{0 \;\; 0 \;\; \cdots \;\; 0\} \qquad\qquad 0 \end{bmatrix}$$

$$+ \frac{m_1}{(1 + m_1 H_{11})} \begin{Bmatrix} \begin{Bmatrix} -H_{21} \\ -H_{31} \\ \vdots \\ -H_{N1} \end{Bmatrix} \\ 1/m_1 \end{Bmatrix} \{\{H_{12} \;\; H_{13} \;\; \cdots H_{1N}\} H_{11}\}. \tag{19}$$

So far, $\mathbf{H}_{11}^{(1)}$ is the only measurement performed and hence, the only available FRF. Therefore, solving equation (19) for the known FRF $H_{11}^{(1)}$

$$\mathbf{H}_{11}^{(1)} = \frac{H_{11}}{(1 + m_1 H_{11})} \Rightarrow H_{11} = \frac{\mathbf{H}_{11}^{(1)}}{(1 - m_1 \mathbf{H}_{11}^{(1)})}, \tag{20}$$

which is simply equation (13). So far nothing is new. In fact, equation (20) is well known and has been around for many years [2]. However, one also wishes to obtain the remaining FRFs ($H_{12}, H_{13}, \ldots, H_{1N}, H_{22}, H_{23}, \ldots, H_{2N}, H_{33}, H_{34}, \ldots, H_{3N}, \ldots, H_{NN}$) without the effects of any added transducers masses and this corresponds to something considered impossible in the past.

2.2.2. *Second situation—uncoupling of* m_1 *and* m_2

The situation is that illustrated in Figure 5. One must remove the effects of m_1 and m_2. Initially, m_2 is uncoupled; i.e., substructure A is now the set constituted by the original structure X and the extra transducers mass at co-ordinate 1. Co-ordinates i are therefore 1,

3 and 4 and j is 2. Equation (19) now becomes

$$\begin{bmatrix} \begin{bmatrix} \mathbf{H}_{11}^{(1,2)} & H_{13}^{(1,2)} & \cdots & H_{1N}^{(1,2)} \\ H_{31}^{(1,2)} & H_{33}^{(1,2)} & \cdots & H_{3N}^{(1,2)} \\ \vdots & \vdots & & \vdots \\ H_{N1}^{(1,2)} & H_{N3}^{(1,2)} & \cdots & H_{NN}^{(1,2)} \end{bmatrix} & \begin{Bmatrix} \mathbf{H}_{12}^{(1,2)} \\ H_{32}^{(1,2)} \\ \vdots \\ H_{N2}^{(1,2)} \end{Bmatrix} \\ \{\mathbf{H}_{21}^{(1,2)} \quad H_{23}^{(1,2)} \quad \cdots \quad H_{2N}^{(1,2)}\} & H_{22}^{(1,2)} \end{bmatrix} = \begin{bmatrix} \begin{bmatrix} \mathbf{H}_{11}^{(1)} & H_{13}^{(1)} & \cdots & H_{1N}^{(1)} \\ H_{31}^{(1)} & H_{33}^{(1)} & \cdots & H_{3N}^{(1)} \\ \vdots & \vdots & & \vdots \\ H_{N1}^{(1)} & H_{N3}^{(1)} & \cdots & H_{NN}^{(1)} \end{bmatrix} & \begin{Bmatrix} H_{12}^{(1)} \\ H_{32}^{(1)} \\ \vdots \\ H_{N2}^{(1)} \end{Bmatrix} \\ \{0 \quad 0 \quad \cdots \quad 0\} & 0 \end{bmatrix}$$

$$+ \frac{m_2}{(1 + m_2 H_{22}^{(1)})} \begin{Bmatrix} \begin{Bmatrix} -H_{12}^{(1)} \\ -H_{32}^{(1)} \\ \vdots \\ -H_{N2}^{(1)} \end{Bmatrix} \\ 1/m_2 \end{Bmatrix} \{\{H_{21}^{(1)} \quad H_{23}^{(1)} \quad \cdots H_{2N}^{(1)}\} \, H_{22}^{(1)}\}. \tag{21}$$

In this case, $\mathbf{H}_{11}^{(1,2)}$, $\mathbf{H}_{12}^{(1,2)}$, $(=\mathbf{H}_{21}^{(1,2)})$ and $\mathbf{H}_{11}^{(1)}$, are known from measurements (note again that the superscripts represent, within brackets, the co-ordinates where there are added masses). So,

$$H_{11}^{(1,\,2)} = H_{11}^{(1)} - \frac{m_2 (H_{12}^{(1)})^2}{(1 + m_2 H_{22}^{(1)})},$$

$$H_{12}^{(1,\,2)} = \frac{H_{12}^{(1)}}{(1 + m_2 H_{22}^{(1)})}, \tag{22}$$

and it follows that

$$H_{12}^{(1)} = \frac{(H_{11}^{(1)} - H_{11}^{(1,\,2)})}{m_2 H_{12}^{(1,\,2)}},$$

$$H_{22}^{(1)} = \frac{(H_{12}^{(1)} - H_{12}^{(1,\,2)})}{m_2 H_{12}^{(1,\,2)}}. \tag{23}$$

These are intermediate FRFs that will be needed in the following steps. Now, m_1 must be uncoupled. This situation has already been treated. It corresponds to expression (19), taking into account that $H_{12}^{(1)}$ and $H_{22}^{(1)}$ are already known from equation (23). Thus,

$$H_{12}^{(1)} = \frac{H_{12}}{(1 + m_1 H_{11})},$$

$$H_{22}^{(1)} = H_{22} - \frac{m_1 (H_{12})^2}{(1 + m_1 H_{11})}, \tag{24}$$

and therefore,

$$H_{12} = (1 + m_1 H_{11}) H_{12}^{(1)}, \tag{25}$$

$$H_{22} = H_{22}^{(1)} + m_1 H_{12} H_{12}^{(1)}. \tag{26}$$

It is not only obvious that the transfer FRF H_{12} was obtained by cancelling the effect of both added masses m_1 and m_2 but also that the direct FRF H_{22} could be obtained without having to measure it.

2.2.3. *Third situation—uncoupling of m_1, m_2 and m_3*

The situation is now that illustrated in Figure 6. One must remove the effects of m_3, m_2 and m_1 following a sequential procedure similar to the one just described. Uncoupling m_3, co-ordinates i are 1, 2, 4, …, N and j is 3. Rewriting, conveniently, (18) and solving in a manner similar to the previous ones

$$H_{13}^{(1,2)} = \frac{(H_{11}^{(1,2)} - H_{11}^{(1,2,3)})}{m_3 H_{13}^{(1,2,3)}},$$

$$H_{23}^{(1,2)} = \frac{(H_{12}^{(1,2)} - H_{12}^{(1,2,3)})}{m_3 H_{13}^{(1,2,3)}}, \tag{27}$$

$$H_{33}^{(1,2)} = \frac{(H_{13}^{(1,2)} - H_{13}^{(1,2,3)})}{m_3 H_{13}^{(1,2,3)}},$$

where all the FRFs on the right-hand side have been measured or are known from the previous calculations. For the uncoupling of m_2, the second situation is repeated, described by expression (21), now having knowledge of the FRFs in equations (27).

Thus,

$$H_{13}^{(1)} = H_{13}^{(1,2)} + m_2 H_{12}^{(1)} H_{23}^{(1,2)},$$

$$H_{23}^{(1)} = (1 + m_2 H_{22}^{(1)}) H_{23}^{(1,2)}, \tag{28}$$

$$H_{33}^{(1)} = H_{33}^{(1,2)} + m_2 H_{23}^{(1)} H_{23}^{(1,2)}.$$

At this stage, the next step to be performed is the cancellation of mass m_1, which is nothing but the first situation again. The final results are given by

$$H_{13} = (1 + m_1 H_{11}) H_{13}^{(1)},$$

$$H_{23} = H_{23}^{(1)} + m_1 H_{12} H_{13}^{(1)}, \tag{29}$$

$$H_{33} = H_{33}^{(1)} + m_1 H_{13} H_{13}^{(1)}.$$

Again, it is obvious that the mass cancellation procedure yielded the unmeasured FRFs H_{23} and H_{33}. Proceeding until the problem for all the other sets of measurements is solved, is just a matter of implementing the appropriate calculations.

It has, therefore, been shown that it is possible not only to cancel all the added transducer masses but also to determine the whole FRF matrix from measurements based on a single column (or a single row). The example presented seems to be clear enough to understand the proposed procedure. Observation of the intermediate as well as the final expressions reveals their recursive nature and their similarity, making the whole procedure simple to generalize to any number N of d.o.f.s and to write it in a systematic way. Consequently, the procedure is easy to program as a small computer subroutine, as has been shown in reference [5] where its simplicity is stressed.

3. EXAMPLE OF APPLICATION

In order to analyze the performance of the proposed technique, a very simple numerical example will be used: a 2-d.o.f. system, with hysteretic damping, as shown in Figure 8. The masses simulating the transducers (m_1 and m_2) were assumed as 2 kg each. The purpose of using such "heavy" transducers is to guarantee that the FRFs corresponding to the example will show clearly (in the graphical display) the influence of the transducers' masses on the "experimental" results.

First, a data set of all the FRF receptance curves was obtained for the original system (without extra masses m_1 and m_2). These curves constitute the target the exact FRFs and are used only for comparison purposes. The second step was to derive the data set of "measured" receptance FRFs ($\alpha_{11}^{(1)}$, $\alpha_{11}^{(1,2)}$ and $\alpha_{12}^{(1,2)}$). The mass cancellation procedure was then applied to this set of "measurements" and the final results were compared with the set of target curves originally derived. Figures 9–11 summarize the procedures presenting the FRF curves superimposed to that the performance of the method can be observed. It is clear that the mass cancellation procedure allowed for a perfect recovery of the α_{11} and α_{12} receptances as well as the derivation of the unmeasured receptance curve α_{22}. Repeating the

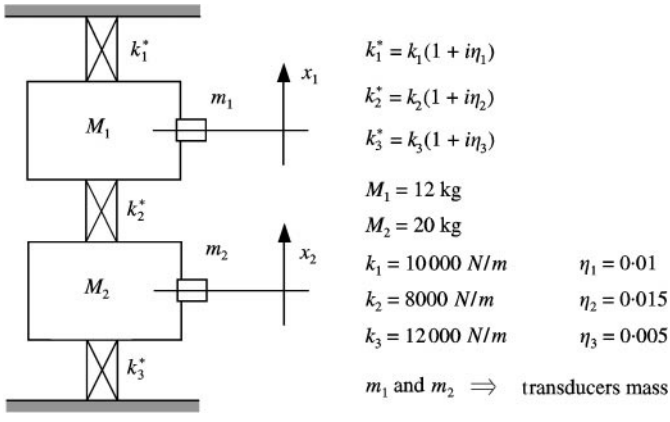

Figure 8. Two d.o.f.s numerical example.

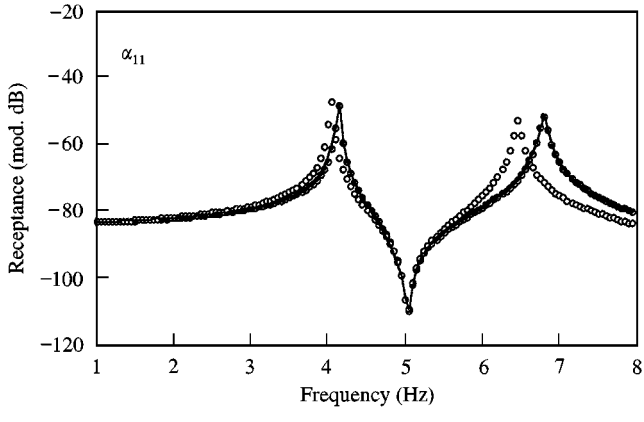

Figure 9. "Measured" and derived point receptance α_{11}, compared with the exact curve: ——, exact; ○, "measured", ●, derived.

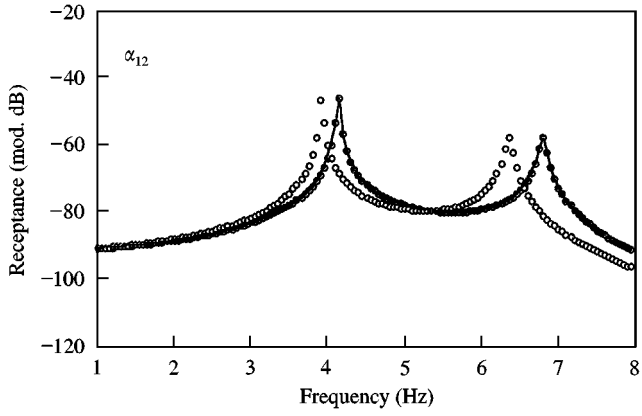

Figure 10. "Measured" and derived transfer receptance α_{12}, compared with the exact curve: ——, exact; ○, "measured", ●, derived.

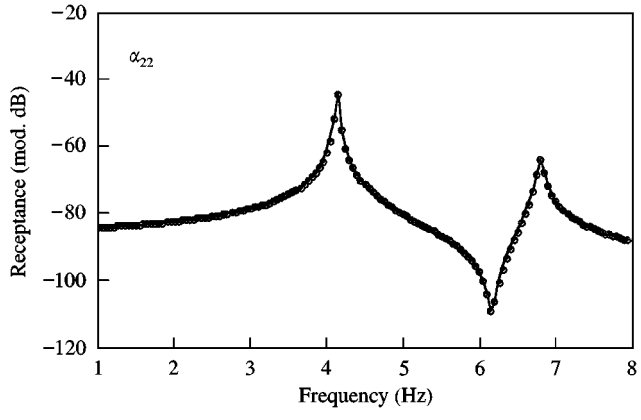

Figure 11. Derived point receptance α_{22}, compared with the exact curve: ——, exact; ●, derived.

procedure with different values of the additional "transducers" masses showed no deviation of the expected results (even with m_1 and/or m_2 as low as 0·2 g).

Despite this extremely good performance, it cannot be forgotten that the method can only be of interest if its application to real data also performs well. It was therefore decided to repeat the previous performance check using the same data and polluting them with random errors. The use of polluted data are meant to simulate real experimental results. Figures 12–14 show the results after applying a $\pm 10\%$ random error to the real and imaginary parts of the receptance data.

It is obvious, from Figure 12, that the cancellation of m_1 yields good results. This was known from past experience, as cancellation of the transducer mass for a point FRF is common knowledge [2]. However, it is immediately apparent that the cancellation procedure is extremely sensitive to errors when the other FRFs are taken into account. In the case of Figure 13, it can be seen that only the region between the two resonance frequencies is acceptable. In the case of Figure 14, the whole FRF tends to be unacceptable.

The previous results are very disappointing as both the cancellation exercise and the objective of deriving a point FRF that had not been measured previously (the ultimate goal

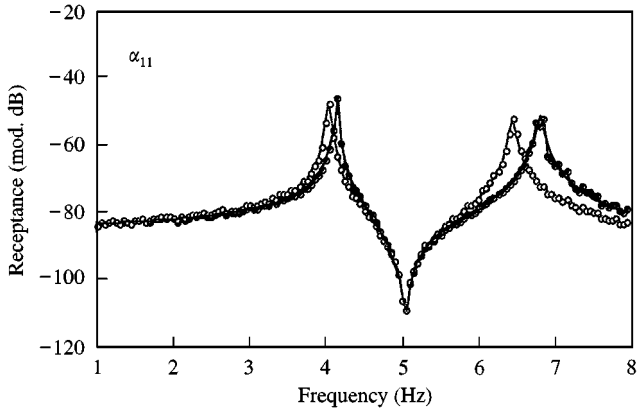

Figure 12. "Measured" and derived point receptance α_{11}, compared with the exact curve (data polluted with $\pm 10\%$ random error): ——, exact; —○—, "measured", —●—, derived.

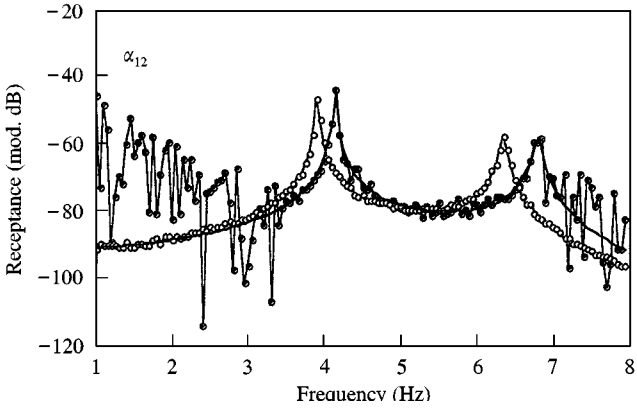

Figure 13. "Measured" and derived point receptance α_{12}, compared with the exact curve (data polluted with $\pm 10\%$ random error): ——, exact; —○—, "measured", —●—, derived.

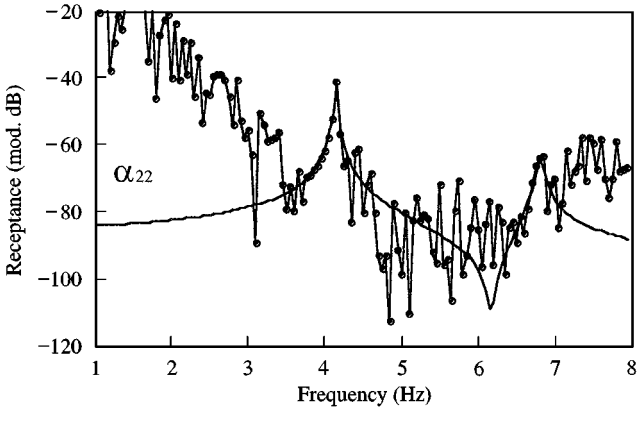

Figure 14. Derived point receptance α_{22}, compared with the exact curve (data polluted with $\pm 10\%$ random error): ——, exact; —●—, derived.

of the method), shows such a dependency on measurement errors that its use with real data cannot be envisaged unless this problem can be solved.

The first idea was to apply identification procedures to all the measured curves identifying modal parameters from the polluted FRFs and regenerating the data would yield smooth curves and, hopefully, better results. Figures 15–17 show what has been achieved. As expected α_{11} yields no problems. However, results get worse when the other two curves are taken into consideration.

It is important to stress here that it is also possible to try to improve the previously derived curves by means of identification procedures. However, in the particular case of α_{22}, it could be seen that improvements could be obtained because the exact curve was known beforehand. In a real situation, this would not be possible and therefore, this type of exercise would not be meaningful.

Thus, despite the fact that it is possible to improve the results using identification procedures, two problems cannot be avoided: (i) the accuracy of the identification procedure is now of great importance; and (ii) in real cases there is no prior knowledge of curves such

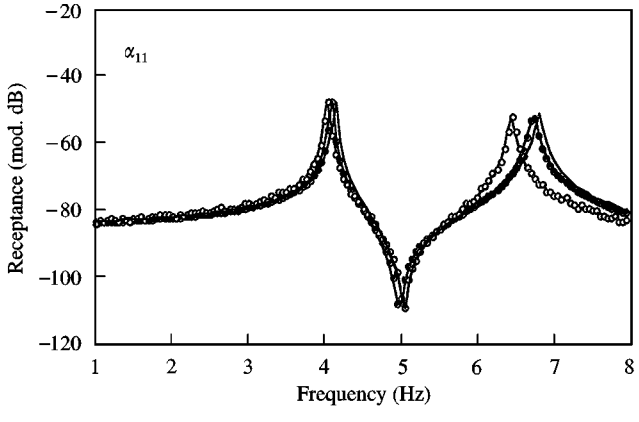

Figure 15. "Measured" and derived point receptance α_{11}, compared with the exact curve (original data were polluted with $\pm 10\%$ random error and subsequently identified): ——, exact; —○—, "measured", —●—, derived.

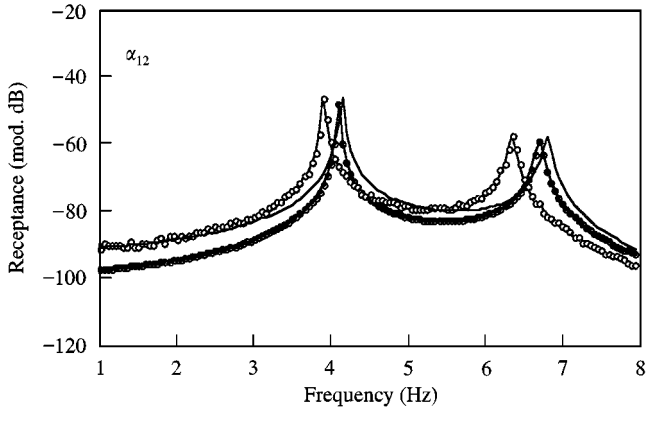

Figure 16. "Measured" and derived transfer receptance α_{12}, compared with the exact curve (original data were polluted with $\pm 10\%$ random error and subsequently identified): ——, exact; —○—, "measured", —●—, derived.

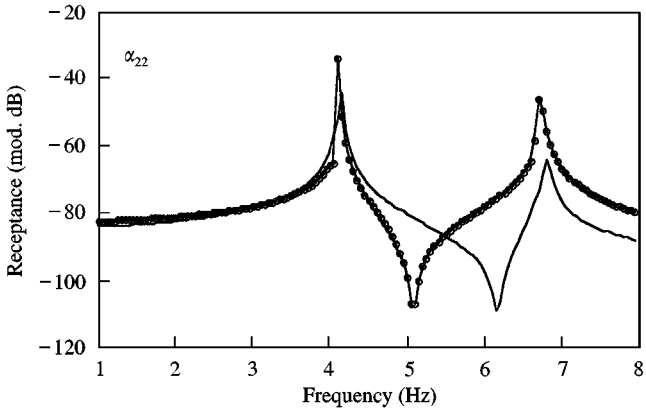

Figure 17. Derived point receptance α_{22}, compared with the exact curve (original data were polluted with $\pm 10\%$ random error and subsequently identified). ——, exact; —●—, derived.

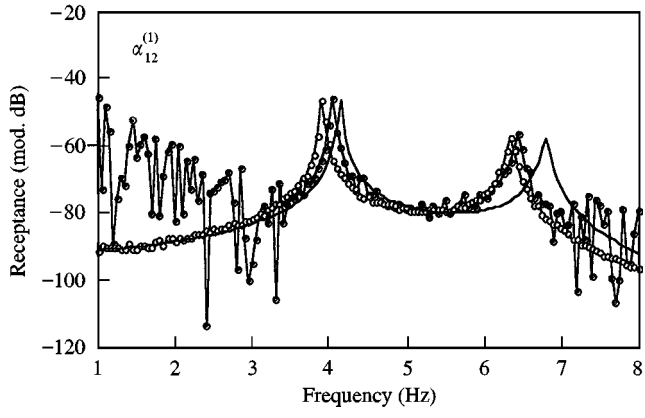

Figure 18. "Measured" receptance $\alpha_{12}^{(1,2)}$ and derived receptance $\alpha_{12}^{(1)}$, compared with the exact curve (data polluted with $\pm 10\%$ random error): ——, exact α_{12}; —○— "measured" $\alpha_{12}^{(1,2)}$, —●—, derived $\alpha_{12}^{(1)}$.

as α_{22} and therefore the performance of the method cannot be evaluated. Moreover, it must be kept in mind that replacing the originally measured curves by smoother FRFs based on equation (7) with the identified modal characteristics, reintroduces the problem of the inconsistency of the residual terms; this is precisely what it was intended to avoid.

Re-analyzing the proposed mass-cancellation method, it becomes obvious that the errors shown in Figures 13 and 14 are the consequence of an error growth contained in the procedure. This is apparent if the intermediate calculations are examined. Equations such as equation (23) contain, in the numerator, a difference between two quantities that are similar in value and already affected by errors. As a consequence, the difference may be of the same order or smaller than the data errors. In fact, plotting the curve $\alpha_{12}^{(1)}$ (also an FRF that was never measured) shows that this intermediate calculation step yields already unacceptable results (Figure 18). Figure 19 shows the reason for this: above and below the two resonances the two polluted curves are almost identical and therefore the derivation of $\alpha_{12}^{(1)}$ will yield poor results in these regions. As a consequence, the subsequent procedure steps will obviously yield unacceptable results as well, and the method fails in its objectives.

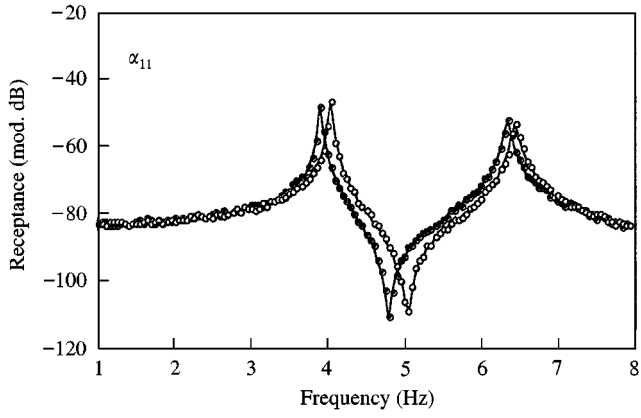

Figure 19. Comparison of the two FRFs whose difference is needed in order to calculate $\alpha_{12}^{(1)}$: —○—, derived $\alpha_{11}^{(1)}$, —●—, "measured" $\alpha_{11}^{(1,2)}$.

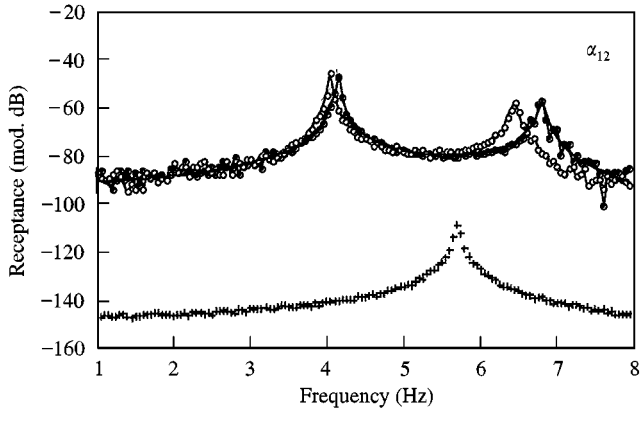

Figure 20. Derivation of α_{12} using a stiff spring to modify $\alpha_{12}^{(1,2)}$ (data polluted with $\pm 10\%$ random error): ——, exact; +, "measured" $\alpha_{12}^{(1,2)}$; —○—, derived $\alpha_{12}^{(1)}$; —●—, derived α_{12}.

On the other hand, in the intermediate region, this type of situation does not occur and results tend to be more reasonable.

Having found the reasons for the errors, a possible solution was immediately apparent: it is imperative that the intermediate calculations, where differences of FRFs are taken, do not yield poor results. One way of solving this problem is to modify one of the curves in order to obtain differences that are larger than the errors.

From examination of equations (23) it can be concluded that introducing a modification at co-ordinate 1 will affect both curves in a similar manner whereas introducing a modification at co-ordinate 2 will only modify one of the curves. Following this reasoning it was decided to modify $\alpha_{11}^{(1,2)}$ artificially by incorporating in the test set-up a stiff spring connecting co-ordinate 2 to ground. The effect of this stiff spring was subsequently cancelled out using the same cancellation procedure as used for the mass. Figures 20 and 21 show the results that were obtained.

There is now a dramatic improvement of the FRFs when compared with what was obtained previously. As these are the final curves, it is always possible to smooth them by

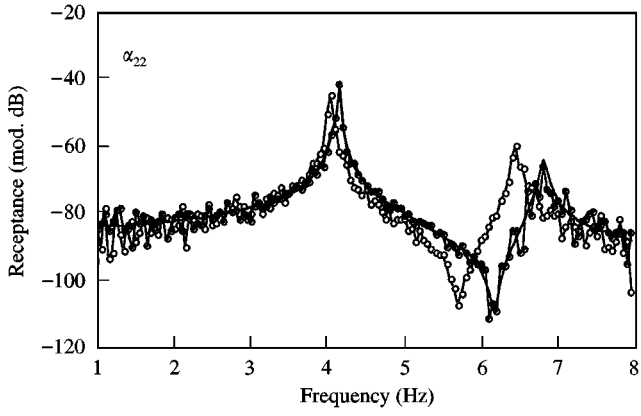

Figure 21. Derivation of α_{22} using a stiff spring to modify $\alpha_{12}^{(1,2)}$: ——, exact; —●—, "measured", —○—, derived $\alpha_{22}^{(1)}$.

means of identification procedures. If, instead of a stiff spring, a very large mass was used (increasing m_2, for example), the results would be very similar.

It seems therefore that the problem was solved given the fact that the results are now reasonable. However, one must bear in mind the feasibility of this solution in practice. The improvement was due to connecting co-ordinate 2 to ground (or to a large mass) by using a stiff spring. Looking at equations (19) and (21), it is obvious that if the modification was to be done by coupling a spring to co-ordinate 1, this could be performed numerically because $\alpha_{11}^{(1)}$ is a known curve. As, in a real situation, the starting point would be having no knowledge of $\alpha_{22}^{(1,2)}$, this connection cannot be performed numerically. This means that measurements of $\alpha_{11}^{(1,2)}$ and $\alpha_{12}^{(1,2)}$ must actually take place with a real stiff spring connecting co-ordinate 2 to ground in the experimental set-up. Alternatively, a similar result could be obtained using a large mass attached to co-ordinate 2. However, incorporating a large mass would be extremely difficult (if not impossible). So, in most cases, to incorporate the spring or a stiff stinger will be more feasible.

It must be noted that this discussion has been centered on a 2-d.o.f. example. As shown at the beginning of the paper, the number of intermediate calculations may grow rapidly with the number of d.o.f.s. For systems larger than the 2-d.o.f. system presented one can expect the problem to be more poorly conditioned. Extending the proposed solution to a larger number of d.o.f.s will nevertheless be possible.

Finally, it must be stressed that the proposed test schedule (or any other alternative sequence leading to the same final objective) tends to be time consuming and therefore, there is always a high probability of change to the underlying (base) structure (suspension, alignment of shaker, etc.) that would add systematic errors to the measured FRFs as well as the random errors noted. Application of this technique to a real structure must therefore be done with very special care in the experimental procedures.

4. CONCLUSIONS

It was shown that, contrary to common belief, it is possible, theoretically, to cancel the added transducer masses in transfer measurements. A procedure was proposed that fulfills this objective. In addition, unmeasured FRFs could be derived, showing that knowledge of a single column (or row) of the FRF matrix is sufficient to derive the complete matrix even

when incomplete models are used. However, the proposed method showed extreme sensitivity to errors in the original data. In principle, this would preclude its use in real cases. A possible solution to this problem has been proposed and some results have been presented, showing its good performance by dramatically improving the final results. The proposed solution implies the use of a stiff spring in order to further modify some of the measured FRFs.

REFERENCES

1. N. M. M. Maia, J. M. M. Silva *et al* 1997 *Theoretical and Experimental Modal Analysis*. England: Research Studies Press Ltd., 1998 re-print.
2. D. J. Ewins 1984 *Modal Testing*: *Theory and Practice*. England: Research Studies Press Ltd.
3. M. L. M. Duarte 1996 *Ph.D. Thesis*, *London*: *Imperial College of Science*, *Technology and Medicine*. Experimentally-derived structural models for use in further dynamic analysis.
4. K. G. McConnell 1995 *Vibration Testing Theory and Practice*. New York: John Wiley & Sons Inc.
5. J. M. M. Silva, N. M. M. Maia and A. M. R. Ribeiro 1997 *Proceedings of the XVth IMAC*, 1431–1439, Orlando, U.S.A. Some applications of coupling/uncoupling techniques in structural dynamics—Part 1: solving the mass cancellation problem.
6. N. M. M. Maia, J. M. M. Silva and A. M. R. Ribeiro 1997 *Proceedings of the XVth IMAC*, 1440–1452, Orlando, U.S.A. Some applications of coupling/uncoupling techniques in structural dynamics—Part 2: generation of the whole FRF matrix from measurements on a single column—the mass uncoupling method (MUM).
7. M. R. Ashory 1998 *Proceedings of the XVIth IMAC*, 815–828, CA: U.S.A. Correction of mass-loading effects of transducers and suspension effects in modal testing.
8. G. W. Skingle 1989 *Ph.D. Thesis*, *London*: *Imperial College of Science*, *Technology and Medicine*. Structural Dynamic Modification Using Experimental Data.